

DESY 97-115
hep-ph/9706399

Instanton Phenomenology at HERA*

A. Ringwald and F. Schrempp

DESY, Notkestr. 85, D-22603 Hamburg, Germany

Abstract

This talk describes the physics input of QCDINS, a Monte Carlo event generator for QCD-instanton induced scattering processes in deep-inelastic scattering.

*Talk presented at the 5th International Workshop on Deep-Inelastic Scattering and QCD (DIS 97), Chicago, April 1997; to be published in the Proceedings (AIP).

Hard scattering processes in strong interactions are successfully described by perturbative QCD. However, perturbation theory does not exhaust all possible hard scattering processes: Instantons [1], non-perturbative fluctuations of the gluon fields, induce hard processes which are absent in perturbative QCD. Deep-inelastic scattering (DIS) at HERA offers a unique window to detect these processes through their characteristic multi-particle final-state signature [2]. A Monte-Carlo generator for instanton-induced events in DIS, QCDINS, interfaced with HERWIG, has been developed [3] which enabled the H1 Collaboration to place first experimental upper limits on the cross-section [4] and which allows for the elaboration of dedicated search strategies [5]. The purpose of this talk is to outline the basic physics input of QCDINS and its built-in features, characteristic for the underlying instanton mechanism. Further details about the theoretical background [6] and ongoing experimental searches [7] appear elsewhere in these proceedings.

In order to appreciate the notion of instanton-induced scattering processes, let us recall that scattering amplitudes are derived via analytic continuation and LSZ reduction from Euclidean Green's functions, which in turn can be represented by a path integral,

$$\frac{1}{Z} \int [dA][d\psi][d\bar{\psi}] A_\mu(x_1) \dots \psi(x_i) \dots \bar{\psi}(x_n) \exp\{-S[A, \psi, \bar{\psi}]\}. \quad (1)$$

The perturbative scattering amplitudes are obtained from an expansion of Eq. (1) about the *perturbative-vacuum solution*, i.e. vanishing gluon fields, $A_\mu^{(0)} = 0$, and vanishing quark fields, $\psi^{(0)} = \bar{\psi}^{(0)} = 0$, with vanishing Euclidean action $S^{(0)} = 0$. This expansion can be summarized by the familiar Feynman rules which construct the perturbative scattering amplitudes in terms of propagators and vertices as a power-series in the strong coupling α_s (see Fig. 1 (left)).

The *instanton* $A_\mu^{(I)}(x)$ is a *non-trivial solution* of the Euclidean gluon-field equations and thus a non-trivial local minimum of the Euclidean action with $S^{(I)} = 2\pi/\alpha_s$. Instanton-induced scattering amplitudes, being derived from an expansion of Eq. (1) about the instanton, can be constructed according to modified Feynman rules, which involve, in addition to the propagators (in the I -background) and vertices (in the I -background) also the classical fields (see Fig. 1 (right)). Instanton-induced scattering amplitudes are always exponentially suppressed at weak coupling, $\propto \exp\{-2\pi/\alpha_s\}$.

In QCD with massless quarks, usual perturbation theory and instanton perturbation theory describe two distinct classes of processes: In usual

perturbation theory, quarks are coupled to gauge fields only via vector couplings, which *conserve chirality* (Q_5). Thus quarks always appear in pairs with net chirality zero (see Fig. 1 (left)) and chirality is conserved to all orders. In instanton-perturbation theory, on the other hand, only scattering amplitudes for processes which *violate chirality* by $\Delta Q_5 = 2n_f$ units receive non-vanishing contributions [8]. This is due to the fact that the classical quark solutions always appear in pairs with net chirality two (see Fig. 1 (right)).

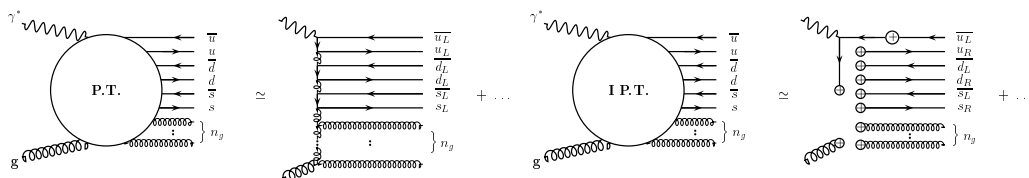


Figure 1: Tree amplitudes for γ^*g scattering processes, in which all light quark flavors are produced. Left: Usual perturbation theory. Right: Instanton-perturbation theory. Lines ending with a blob stand for classical right-handed quark ($\psi_R^{(I)}$) and anti-quark ($\overline{\psi_L^{(I)}}$) solutions; line with a blob in the middle denotes the quark propagator in the I -background; curly lines ending with a blob stand for classical instanton gluon fields ($A_\mu^{(I)}$).

The Monte-Carlo simulation of I -induced events proceeds in three steps. First, quasi-free partons are produced by QCDINS with the distributions prescribed by the hard process matrix elements. Next, these primary partons give rise to parton showers, as described by HERWIG. Finally, the showers are converted into hadrons, again within HERWIG.

The momentum-space structure of I -induced hard processes in γ^*g scattering is shown in Fig. 2 (left). As is already suggested by the form of the leading-order matrix elements in Fig. 1 (right), the amplitudes factorize into a product of an effective γ^*qq^* vertex [9], denoted by a blob in Fig. 2 (left), times matrix elements for I -induced partonic subprocesses, $q^*g \rightarrow (2n_f - 1)q + n_g g$, denoted by a blob with an index “ I ”. It turns out that the most important kinematical variables determining the final state properties of I -induced events are the virtuality of the off-shell quark q^* , $Q'^2 \equiv -q'^2 \geq 0$, and the Bjorken scaling variable of the q^*g subprocess, $x' \equiv Q'^2/(2p \cdot q')$. Therefore let us discuss their distributions first.

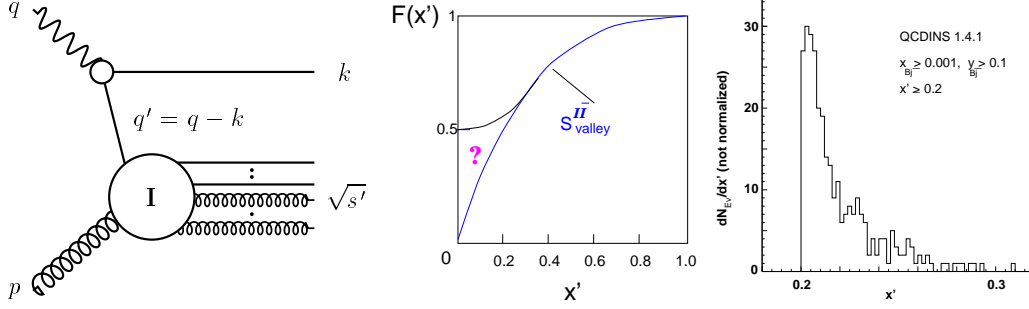


Figure 2: Left: Momentum-space structure of I -induced partonic processes in γ^*g scattering. Middle: The holy-grail function $F(x')$. Right: x' distribution from QCDINS.

To this end, we square the amplitudes in Fig. 2 (left) and sum over all final state partons to construct the I -induced hard-scattering partonic total cross-section or structure function. It can be shown [9] that the initial state collinear singularities, occurring when $Q^2 \rightarrow 0$, can be consistently absorbed into the parton distribution functions f_k , such that the I -induced contribution to the nucleon-structure function is obtained in the familiar convolution form,

$$F_2^{(I)}(x_{Bj}, Q^2) = \sum_k \int_{x_{Bj}}^1 \frac{dx}{x} f_k \left(\frac{x_{Bj}}{x}, \mu_f^2, \mu^2 \right) \frac{x_{Bj}}{x} \mathcal{C}_{2k}^{(I)} \left(x, \frac{Q^2}{\mu^2}, \frac{\mu_f^2}{\mu^2}, \alpha_s(\mu) \right), \quad (2)$$

where $\mu(\mu_f)$ denotes the renormalization (factorization) scale. The I -contribution to the dominating gluon-coefficient function $\mathcal{C}_{2g}^{(I)}$ in turn, has for large Q^2 the anticipated momentum-space structure [2, 9],

$$\mathcal{C}_{2g}^{(I)} \left(x, \frac{Q^2}{\mu^2}, \frac{\mu_f^2}{\mu^2}, \alpha_s(\mu) \right) \simeq x \sum_q e_q^2 \times \int_x^1 \frac{dx'}{x'} \int_{\mu_f^2}^{Q^2 \frac{x'}{x}} dQ'^2 \frac{3}{16 \pi^3} \frac{x}{x'} \left(1 + \frac{1}{x} - \frac{1}{x'} - \frac{Q'^2}{Q^2} \right) \sum_{n_g} \sigma_{q^*g; n_g}^{(I)} \left(x', Q'^2, \alpha_s(\mu) \right). \quad (3)$$

The essential instanton dynamics and in particular most of the dependence

on x' and Q' is encoded in the I -subprocess total cross section,

$$\sum_{n_g} \sigma_{q^*g; n_g}^{(I)}(x', Q'^2) \simeq \frac{\Sigma(x')}{Q'^2} \left(\frac{4\pi}{\alpha_s(\mu(Q'))} \right)^{21/2} \exp \left[-\frac{4\pi}{\alpha_s(\mu(Q'))} F(x') \right], \quad (4)$$

where the functions $\Sigma(x')$ and $F(x')$ (see Fig. 2 (middle)) are known [10, 2] for $x' \geq x'_{\min} \simeq 0.2 - 0.3$.

We see from Eq. (4) that the summation over the gluon emission has modified the exponential suppression factor by the so-called ‘‘holy-grail’’ function $F(x')$. This exponentiation is due to the fact that every gluon emission brings in a factor of $A_\mu^{(I)} \sim 1/\sqrt{\alpha_s}$ in the exclusive amplitudes (see Fig. 1 (right)), such that [11] $\sigma_{q^*g; n_g}^{(I)} \propto (1/n_g!)(1/\alpha_s)^{n_g} \exp\{-4\pi/\alpha_s\}$.

The holy-grail function $F(x')$ is continuously decreasing from 1 at $x' = 1$ (low q^*g c.m. energy) to 1/2 at $x' \simeq 0.2$ (see Fig. 2 (middle)). The total cross-section is correspondingly exponentially growing with decreasing x' . This is clearly seen in the x' distribution taken from the Monte-Carlo simulation (see Fig. 2 (right)).

Thanks to the chosen renormalization scale, $\mu(Q') = Q'\alpha_s(\mu(Q'))/(4\pi)$, the I -subprocess cross-section (4), as a function of the q^* virtuality Q' , has a peak structure which is clearly reflected by the Q' distribution in Fig. 3 (left). The peak is at around 5 GeV, which is gratifying since it means that even without a lower Q' cut¹ most of the events generated are hard enough in order to justify instanton-perturbation theory [9].

In Fig. 3 (right) we present the resulting I -induced total eP cross-section for HERA, subject to the following cuts: *i*) $x_{\text{Bj}} \geq x_{\text{Bj min}}$, $y_{\text{Bj}} \geq 0.1$ in Eq. (2); *ii*) $x' \geq x'_{\min}$ in the integration of Eq. (3). No cut on Q' has been imposed. It is important to note that lower limits on x' and Q' can be enforced experimentally by cuts on final state momenta¹. The points in Fig. 3 (right) have been taken from the Monte-Carlo simulation (QCDINS 1.4.1). As a check of the Monte-Carlo, we have also analytically integrated Eqs. (2) and (3). The resulting cross-section (lines in Fig. 3 (right)) nicely agrees with the Monte-Carlo result. We refrain from going to even smaller x_{Bj} , say 10^{-4} , since in this case $Q^2 = x_{\text{Bj}} y_{\text{Bj}} S$ would be only of order 1 GeV². It is not clear whether in this case the corrections to Eq. (3), which are not built into QCDINS, can be neglected.

¹A minimum Q' can be enforced by requiring the transverse momentum k_T of the current-quark jet (see Fig. 2 (left)) to be large. A lower x' -cut can be implemented, for example, by requiring $x \equiv Q^2/(Q^2 + s) \gtrsim x'_{\min}$, where s is the γ^*g c.m. energy.

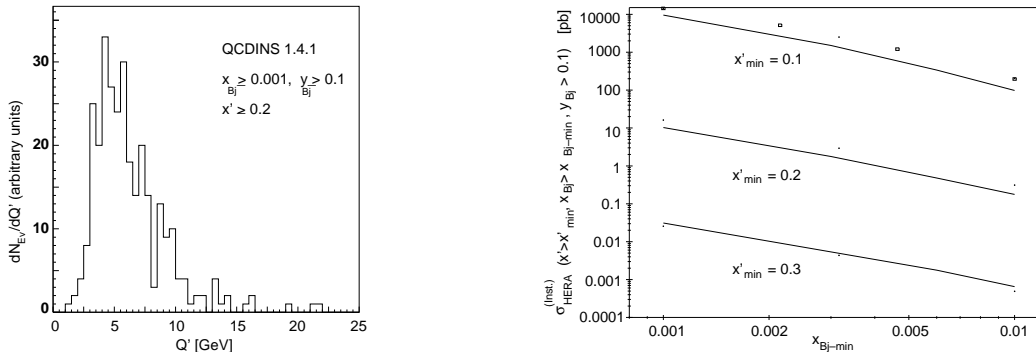


Figure 3: Left: Q' distribution. Right: I -induced total eP cross-section for HERA (preliminary) with various cuts as indicated. Lines: Analytical calculation. Points: Monte-Carlo simulation with QCDINS 1.4.1.

As a benchmark for searches for I -induced events at HERA [4, 7], let us compare the I -induced HERA cross-section from Fig. 3 (right) with the normal DIS HERA cross-section, $\sigma_{\text{HERA}}^{(\text{nDIS})}(x_{Bj} > 10^{-3}, y_{Bj} > 0.1) \simeq 15$ nb. We see that the fraction of I -induced events at HERA, $f^{(I)} \equiv \sigma_{\text{HERA}}^{(I)}/\sigma_{\text{HERA}}^{(\text{nDIS})}$, ranges between

$$0.0002 \% \lesssim f^{(I)} \lesssim 0.1 \% , \quad (5)$$

in the kinematical range $x' > 0.3..0.2$, $x_{Bj} > 10^{-3}$, $y_{Bj} > 0.1$. Note that the published upper limits on the fraction of I -induced events placed by the H1 Collaboration [4] are in the several percent range. An improvement of these limits by an order of magnitude is reported in another talk in this working group [7].

Let us turn now to the final states of I -induced events in DIS. The current quark in Fig. 2 (left) will give rise, after hadronization, to a current-quark jet. The partons from the I -subprocesses, $q^*g \rightarrow (2n_f - 1)q + n_g g$ (see Fig. 2 (left)), on the other hand, are emitted spherically symmetric in the q^*g c.m. system (“ I -c.m. system”). The gluon multiplicities are generated according to a Poisson distribution with mean multiplicity

$$\langle n_g(x', Q') \rangle^{(I)} \simeq \frac{2\pi}{\alpha_s(\mu(Q'))} x'(1-x') \frac{dF(x')}{dx'} , \quad (6)$$

which is of the order of two for $x' \simeq 0.2$, $Q' \simeq 5$ GeV (see Fig. 4 (left)). The total mean parton multiplicity is large, of the order of ten. After hadroniza-

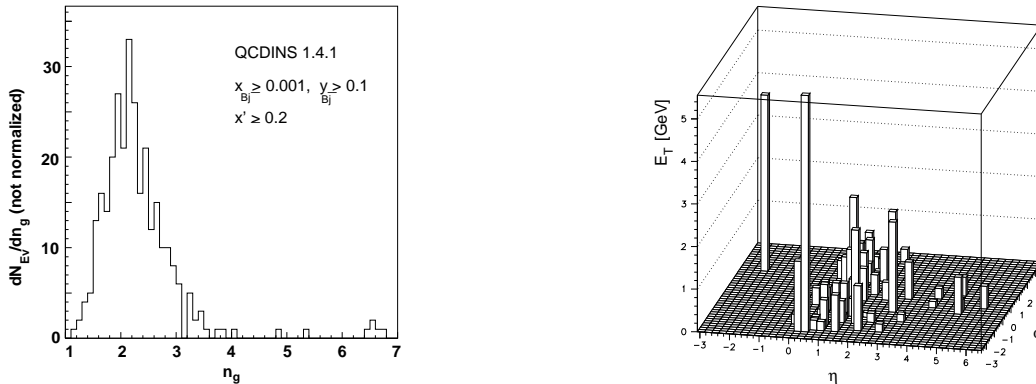


Figure 4: Left: Gluon multiplicity distribution of I -induced events. Right: Lego plot of a typical I -induced event in the HERA-lab system at $x_{Bj} = 10^{-3}$.

tion we therefore expect from the I -subprocess a final state structure reminiscent of a decaying fireball: Production of the order of 20 hadrons, always containing strange and possibly charmed mesons, concentrated in a “band” at fixed pseudorapidity η in the $(\eta, \text{azimuth angle } \phi)$ -plane. Due to the boost from the I -c.m. system to the HERA-lab system, the center of the band is shifted in η away from zero, and its half-width is of order $\Delta\eta = 0.9$, as typical for a spherically symmetric event. The total invariant mass of the I -system, $\sqrt{s'} = Q' \sqrt{1/x' - 1}$, is expected to be in the 10 GeV range, for $x' \simeq 0.2$, $Q' \simeq 5$ GeV. The lego plot of a typical I -induced event shown in Fig. 4 (right) shows that these expectations (current-quark jet; hadronic “band”) are actually borne out from our Monte-Carlo simulation.

Acknowledgements

We would like to thank M. Gibbs and S. Moch for fruitful collaboration and T. Carli for its help in debugging and improving QCDINS.

References

- [1] A. Belavin *et al.*, Phys. Lett. **59B**, 85 (1975).

- [2] A. Ringwald and F. Schrempp, hep-ph/9411217, in: *Quarks '94*, Vladimir, Russia, 1994, eds. D. Grigoriev et al., pp. 170-193;
A. Ringwald and F. Schrempp, DESY 96-203, hep-ph/9610213, to be published in: *Quarks '96*, Proc. 9th Int. Seminar, Yaroslavl, Russia, May 5-11, 1996.
- [3] M. Gibbs, A. Ringwald and F. Schrempp, hep-ph/9506392; in: *Proc. Workshop on Deep Inelastic Scattering and QCD*, Paris, 1995, pp. 341-344;
T. Carli, M. Gibbs, A. Ringwald and F. Schrempp, in preparation.
- [4] S. Aid *et al.*, H1 Collaboration, Nucl. Phys. **B480**, 3 (1996);
S. Aid *et al.*, H1 Collaboration, Zeit. Phys. **C72**, 573 (1996).
- [5] M. Gibbs, T. Greenshaw, D. Milstead, A. Ringwald and F. Schrempp, in: *Proc. Future Physics at HERA*, 1996, Vol. 1, pp. 509-514.
- [6] S. Moch, A. Ringwald and F. Schrempp, these proceedings (WG V).
- [7] T. Carli and M. Kuhlen, these proceedings (WG III).
- [8] G. 't Hooft, Phys. Rev. Lett. **37**, 8 (1976); Phys. Rev. D **14**, 3432 (1976);
Phys. Rev. D **18**, 2199 (1978) (Erratum).
- [9] S. Moch, A. Ringwald and F. Schrempp, DESY 96-202, hep-ph/9609445 and in preparation.
- [10] I. Balitsky and V. Braun, Phys. Lett. **314B**, 237 (1993).
- [11] A. Ringwald, Nucl. Phys. **B330**, 1 (1990);
O. Espinosa, Nucl. Phys. **B343**, 310 (1990).